# QUANTIFYING THE SURFACE RUGGEDNESS OF THE ROCK OUTCROPS BY USING 3D DIGITAL OUTCROP MODELS

**Takumu Nakamura[1], Arata Kioka[2], Yasuhiro Yamada[2]**

**[1] Cooperative Program for Resources Engineering, Graduate School of Engineering, Kyushu University**
**[2] Department of Earth Resources Engineering, Kyushu University**





## ABSTRACT

A recent 3D digitization technology has advanced the development of 3D digital outcrop models (3D-DOMs). Yet, few studies report the effort in extracting the physical properties of rocks from 3D-DOMs. We aim to investigate the relationship between the surface morphology and the physical properties of the rocks at outcrops. First, we created high-resolution Digital Elevation Model (DEM) images with different spatial resolutions from high-resolution 3D-DOMs, and calculated Terrain Ruggedness Index (TRI), Roughness, and Topographic Position Index (TPI). The 3D-DOMs were generated by the drone flyover in the Itoshima Peninsula Coast and the Oga Peninsula Coast. Second, we produced orthoimages using the 3D-DOMs and extracted them to the data in the Hue, Saturation, and Value (HSV) color space. We also newly defined a ruggedness index $G_{TRI}$ by normalizing TRI using the maximum value of TRI. We examined the correlation between HSV color spaces and the ruggedness index $G_{TRI}$. Third, we examined the use of a machine learning model to predict the ruggedness of the orthoimage in the Oga Coast, with the Itoshima Coast data, HSV color space data, and $G_{TRI}$ data as the supervisory data, explanatory variables, and the objective function, respectively.

We found TRI is the most effective index representing the small-spatial scale roughness. Our ruggedness parameter $G_{TRI}$ showed good correlations with those in the HSV color space. Among the good correlations, $G_{TRI}$ showed the best correlation with V, suggesting a correlation between the outcrop ruggedness and V in the orthoimage. We further found that our machine learning model generally reconstructed well the $G_{TRI}$ image of the Oga Coast, with the successful prediction of the presence of relatively large-scale ruggedness such as cracks. The results suggest that our method by integrating the TRI parameters and HSV color spaces acquired from UAV photography can be a powerful method to estimate rock properties.

## INTRODUCTION

Conventional geological surveys require field visits to photograph outcrops and collect rock materials, which limit the survey area to areas accessible to humans. The quality and quantity of geological information obtained during a field survey are affected not only by the subject of the field survey, such as the degree of undulation and the state of preservation of the outcrop surface, but also weather conditions and solar radiation. In addition, the skill level of the researcher describing the outcrop or collecting the sample can also significantly influence the quality of the information. Data obtained from geological surveys are compiled as two-dimensional drawings such as columnar maps or geological maps, or as qualitative geological models, hampering to manage geological information in a 3D and quantitative manner.

Three-dimensional digital outcrop models (3D-DOMs) are now attracting attention as a means of overcoming these problems: by taking aerial photographs with unmanned aerial vehicles (UAVs) and creating a 3D-DOM based on the image data taken. The information acquired by UAVs that can be comparable to the visual information obtained from the outcrops regardless of human accessibility (Blistan et al., 2016). In addition, since the UAV can be equipped with sensors to acquire the necessary information, it is now possible to project the obtained information onto the 3D-DOM and to manage all data by integrating the data obtained from the geological survey into the 3D-DOM. 3D-DOMs are also useful for visualizing logging data (Buckley et al., 2019).

Recently, there are some virtual geology projects that make 3D-DOMs available on the Internet for generating geological models (Nemoto et al., 2002). The 3D-DOMs are freely available on the Internet under Creative Commons Attribution. The 3D-DOMs can be used for analysis and are tools to facilitate the further development of 3D-DOMs as research materials. The 3D-DOMs have been analyzed in various ways and have been used to extract discontinuous geologic structures such as joints, fractures, and faults. However, the analysis of 3D-DOMs has a short history, and there is much room for considering and developing new methods (Bemis et al., 2014).

The 3D-DOMs contain visual information such as outcrop color and morphology created from UAV aerial photography data. Research focusing on the color of outcrops has been quite active, including a study on outcrop image segmentation for selecting areas suitable for Carbon Capture and Storage (Sato et al., 2021). In addition, there is a long tradition of research on morphology as part of geomorphology, a field of natural geography, and on a larger scale, a study on the possibility that local morphological heterogeneity, including roughness and thickness, of subsurface active faults controls fault slip (Yamada et al., 2013). Research has also been conducted at smaller scales, such as the fracture surface of metallic materials, and various studies have pointed out that the uneven morphology of the fracture surface is affected by the type of metal, heat treatment, and degree of processing (Koterazawa, 1987; Lynch & Moutsos, 2006). However, few studies reported medium-scale morphology such as outcrops, and it is thus still unclear whether there is any causal relationship between outcrop ruggedness and the physical properties of the rock. This study has the following three objectives. (1) Investigating the relationship between outcrop surface unevenness and the physical properties of outcrop rocks, by comparing and studying the indices for evaluating unevenness and proposing an optimal quantitative method for evaluating unevenness. (2) Investigating the relationship between outcrop surface color and unevenness obtained from UAVs using orthoimage in HSV color space, for discussing useful indices for studying the relationship between unevenness and rock properties. (3) Examining the feasibility of constructing a machine learning model that can estimate unevenness from individual orthoimages in HSV color space by using their HSV color spaces and unevenness indices.

## Study Areas

Two locations were selected as the study areas for geological and drone surveys: Nogita Coast, Itoshima Peninsula, Fukuoka, Japan (Figure 1) and Unosaki Coast, Oga Peninsula, Akita, Japan (Figure 2).

In the Nogita Coast area, muddy schist and mafic schist of the Sangun metamorphic rocks are distributed in a band between the plutonic rocks. Metamorphic rocks are rocks formed when the minerals and rock properties of source rocks, such as sedimentary rocks, are altered by heat and pressure in the subsurface. Muddy schist is a metamorphic rock formed from sedimentary mudstone that has undergone extensive metamorphism, mainly due to pressure, and has developed a thin, easily fractured schist structure. Outcrops of muddy schist have complex outcrop shapes due to weathering by rain and waves, while outcrops of mafic schist contain fine structures but are exposed as a massive whole. To create a more accurate 3D-DOM, this study focuses on outcrops of mafic schist.

In the Unosaki Coast area, the Onnagawa Formation exposed on the Unosaki Coast is siliceous, extremely hard rocky hard mudstone. The mudstone of the Unosaki Coast is hard because of the large number of diatoms that have accumulated there. The presence of laminae in some hard mudstones suggests that deep oxygenated currents did not flow into the seafloor in Akita during the period when the Onnagawa Formation was deposited. The mudstone containing this preserved organic matter is the source rock for petroleum (Sato et al., 2009). Calcareous nodules are


**Figure 1**: - Aerial view of the Nogita coastal area (Google Earth) and survey sites (red circles in C)


**Figure 2**: - Aerial view of the Unosaki coastal area (Google Earth) and survey sites (red circles in C)

also found in the Onnagawa Formation on the Unosaki Coast. A nodule is a hardened sedimentary rock in which silicic acid and carbonate have been chemically concentrated and precipitated by fossils and sand grains as a nucleus and agglomerated harder than the surrounding host rock. They are generally spherical and have distinct differences in composition from the surrounding host rock. On the Unosaki Coast, calcareous nodules identified by aerial photography with a UAV were the target of the study.

## Methodology

*Create 3D-DOMs and DEM.* UAV-Structure from Motion (SfM)/Multi-view Stereo (MVS) or LiDAR are generally used to create 3D-DOMs. UAV-SfM/MVS is cost-effective and time-efficient on a large scale, while LiDAR is better capability to characterize morphological details (Li et al., 2020). In this study, we used an UAV-SfM/MVS

(Figure 3). UAV-SfM/MVS surveying was conducted using the following procedure to create 3D-DOMs. The entire process was done by manual control, changing the tilt of the gimbal and the angle at which the image was taken because the outcrops were overhanging and there were areas that could not be photographed by autopilot. Even with manual maneuvering, it is possible to construct a 3D model with high distance accuracy and repeatability and a clear extractable cross-section by taking oblique photographs so that the sides of the structure can be seen while being aware of the high overlap and side-wrap rates (Nagaya & Kiku, 2020). By increasing the overlap rate, the outcrop model created by aerial photogrammetry is known to agree accurately when compared to actual measurements of strike and dip (Totake, 2019). Aerial photography for this study was conducted with an overlap ratio of approximately 80%. In addition, the distance between the UAV and the outcrop surface was kept below 1.0 m to improve the resolution of the aerial data. The manual shooting mode required 30 minutes (maximum continuous flight time) for each of the two target areas because of the time required for shooting. In this study, 130 photos and 128 photos were read for the Nogita Coast the Unosaki Coast, respectively, after removing those considered to be of low quality due to blurring. Then, 3D-DOMs of the two target sites were created. The DEM images were created based on respective 3D-DOMs.

*Calculation of each ruggedness index.* Each ruggedness index is calculated based on DEM and uses the eight pixels surrounding the center pixel to calculate the value of the center pixel, as shown in the pixel relationship diagram (Figure 4). $Z_{(i,j)}$ is the value of the representative point of each cell.

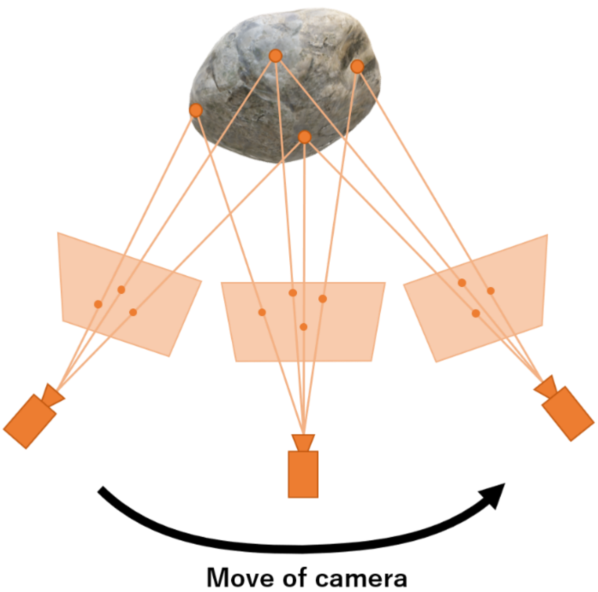


**Figure 3**: - UAV-SfM/MVS overview chart

| | | |
|---|---|---|
| $i-1, j-1$ | $i, j-1$ | $i+1, j-1$ |
| $i-1, j$ | $i, j$ | $i+1, j$ |
| $i-1, j+1$ | $i, j+1$ | $i+1, j+1$ |

**Figure 4**: - Pixel relationship diagram

TRI is the average of the absolute difference in Z coordinate values between the center pixel and its surrounding 8 cells at a grid point. TRI is calculated by (Riley et al., 1999):

$$TRI = \sum_{\alpha,\beta} \frac{|Z_{i+\alpha,j+\beta} - Z_{i,j}|}{8} \tag{1}$$

$Z_{(i,j)}$ : central pixel
α: index (-1, 0, 1)
β: index (-1, 0, 1)

Roughness is calculated by the difference between the largest cell of the center pixel and its surrounding cells and is defined by the following Equation (2).

$$Roughness = \max_{i,j} |Z_{i+\alpha,j+\beta} - Z_{i,j}| \tag{2}$$

$Z_{(i,j)}$ : central pixel
α: index (-1, 0, 1)
β: index (-1, 0, 1)

The TPI is calculated by the difference between the center pixel and the average of its surrounding cells and is defined by the following Equation (3).

$$\mathrm{TPI} = Z_{i,j} - Z_{i+\alpha,j+\beta} \tag{3}$$

$Z_{(i,j)}$ : central pixel
α: index (-1, 0, 1)
β: index (-1, 0, 1)
$\alpha=\beta\neq 0$

*Change in values of each ruggedness index for different resolution of DEM.* The value of each ruggedness index possibly changes depending on the spatial resolution of DEM since it is calculated based on DEM. The following operations were conducted to understand the influence of resolution differences. The spatial resolution was reduced when creating the DEM. The highest resolutions of the DEM at Nogita Coast and Unosaki Coast were $0.607\times10^{-3}$ (m/pix) and $0.472\times10^{-3}$ (m/pix), respectively. DEM images were created by gradually decreasing the resolution from the highest resolution. TRI, Roughness, and TPI were calculated at each resolution.

*Relationship between HSV color space and ruggedness.* HSV color space is a method of expressing color by combining hue (H), saturation (S) and Value (V). Since the HSV color space is similar to the way humans distinguish colors, it is easier to produce colors as people imagine them than the RGB color space. For this reason, the HSV color space is used for color detection in image processing. Orthoimages of the Nogita Coast and Unosaki Coast were converted from RGB color space to HSV color space. The HSV image was separated into H image, S image, and V image. The images are shown together with the original image, H image, S image, and V image (Figure 5) (Figure 6).

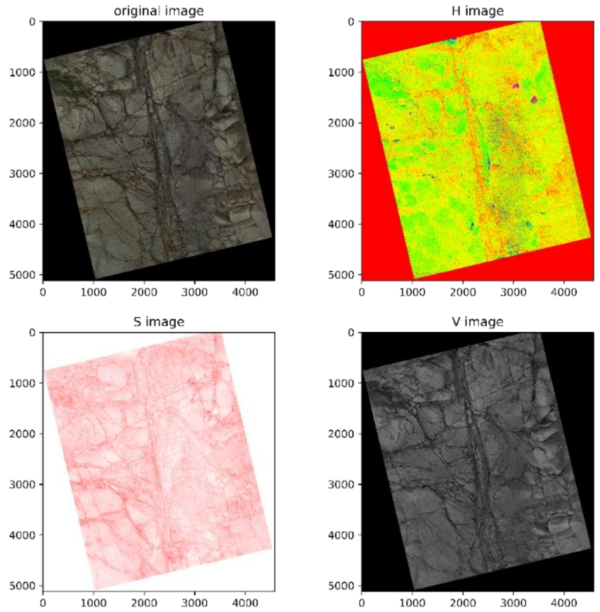


**Figure 5**: - Original image (top left), H image (top right), S image (bottom left) and V image (bottom right) at Nogita Coast (Numbers are pixcel numbers)

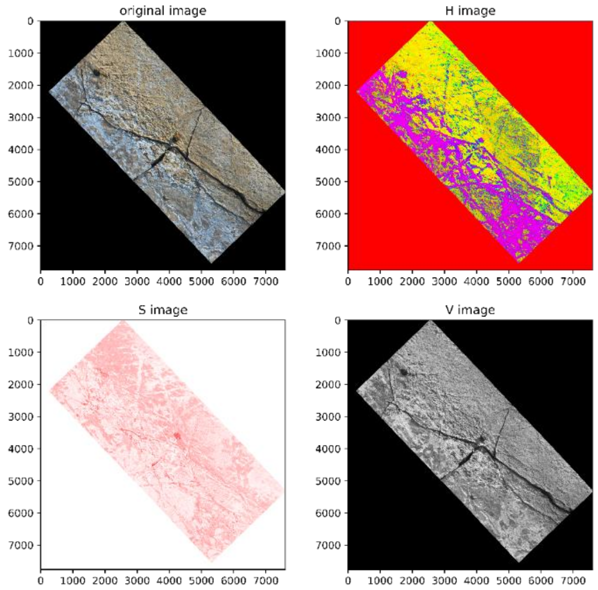


**Figure 6**: - Original image (top left), H image (top right), S image (bottom left) and V image (bottom right) at Unosaki Coast (Numbers are pixcel numbers)

In order to visually compare TRI and HSV images more easily, $G_{TRI}$ was defined in Equation (4) as a ruggedness index. $G_{TRI}$ is calculated based on TRI, and the value decreases as TRI increases.

$$G_{TRI} = \left(\frac{\max(TRI) - TRI}{\max(TRI)}\right) \times 255 \qquad (4)$$

We considered the relationship between HSV color space and the ruggedness using $G_{TRI}$.

*Quantifying $G_{TRI}$ by machine learning model.* We created machine learning model to quantify $G_{TRI}$ of Unosaki Coast. In this machine learning model, H, S, and V in the HSV color space were used as explanatory variables, and $G_{TRI}$ was used as the objective variable. Multilayer perceptron (MLP) was used for the machine learning model (Figure 7).

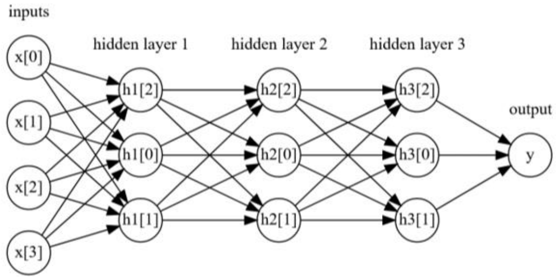


**Figure 7**: - Multilayer perceptron

MLP is a type of Feed-forward Neural Network (FfNN), and it is the gateway to understand deep learning. The MLP is constructed from an input layer, one or more threshold logic unit (TLU) layers, called hidden layers, and one final TLU layer, called the output layer. The TLU computes a weighted sum of the inputs, applies a step function to the sum, and outputs the result. Using data at Nogita Coast as teaching data, a model was constructed to quantify $G_{TRI}$ values at Unosaki Coast based on H, S, and V values at Unosaki Coast (Figure 8).

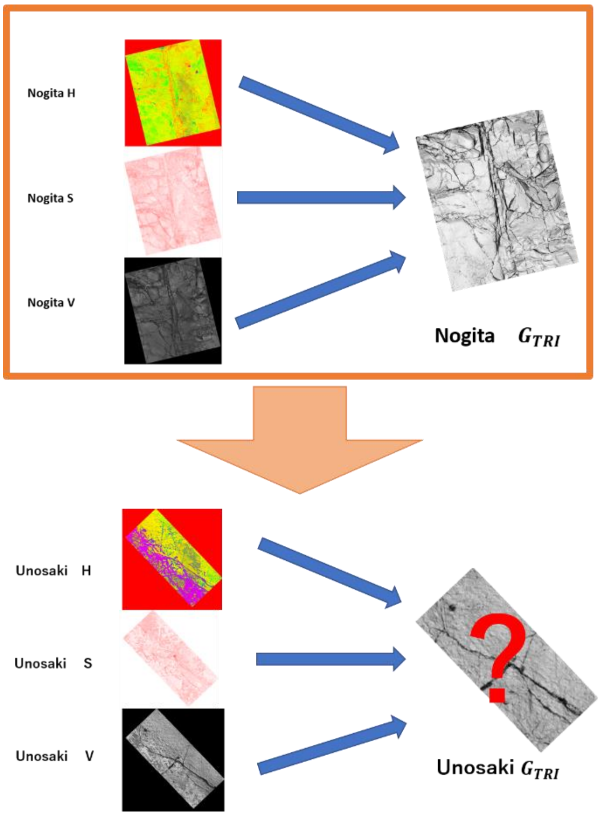


**Figure 8**: - Machine learning model for estimating $G_{TRI}$

## Results

*Change in values of respective ruggedness index with different spatial resolution of DEM.* Figure 9 shows the change of TRI at different spatial resolutions at Nogita Coast. The blue plots are the TRI values and the orange plots are The average values of TRI. The average values of TRI increase monotonically with increasing resolution. Figure 10 shows the change of Roughness at different resolutions at Nogita Coast. The average values of Roughness increase monotonically with increasing resolution, similar to TRI. Figure 11 shows the change of TPI at different resolutions at Nogita Coast. The average values are constant around zero for the most part. It shows large negative values around the point where the resolution became low.

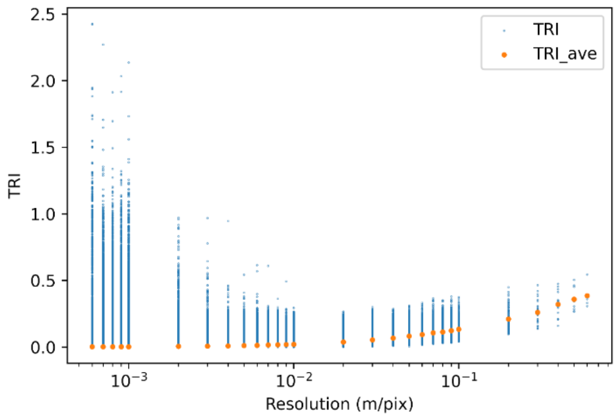


**Figure 9**: - Change of TRI values at different resolutions at Nogita Coast

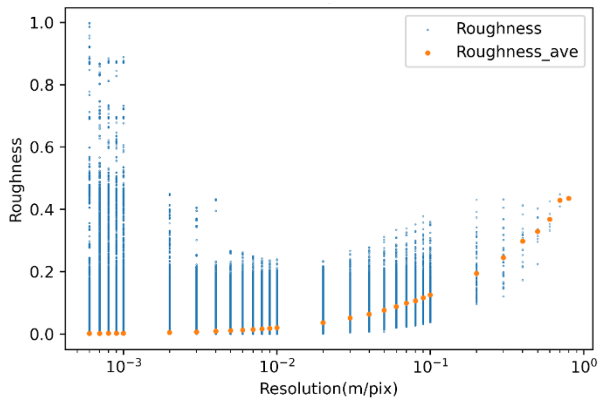


**Figure 10**: - Change of Roughness values at different resolutions at Nogita Coast

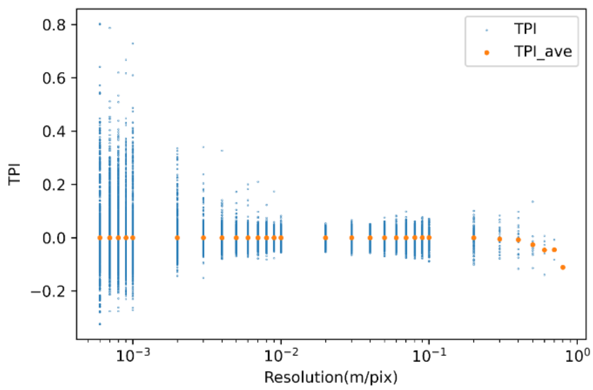


**Figure 11**: - Change of TPI values at different resolutions at Nogita Coast

Figure 12 shows the change of TRI at different resolutions at Unosaki Coast. The blue plots are the TRI values and the orange plots are the average values of TRI. Figure 13 shows the change of Roughness at different resolutions at Unosaki Coast. Figure 14 shows the change of TPI at different resolutions at Unosaki Coast. Unosaki Coast results were very similar to Nogita Coast results. However, in the TPI graph, The average values of TPI were always close to zero.

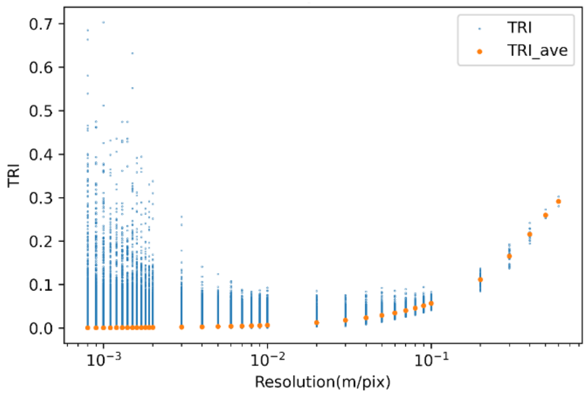


**Figure 12**: - Change of TRI values at different resolutions at Unosaki Coast

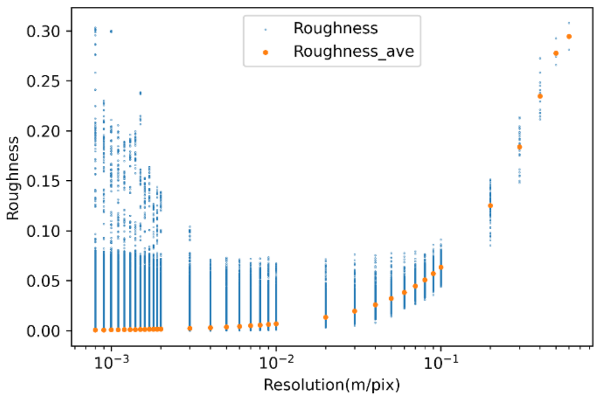


**Figure 13**: - Change of Roughness values at different resolutions at Unosaki Coast

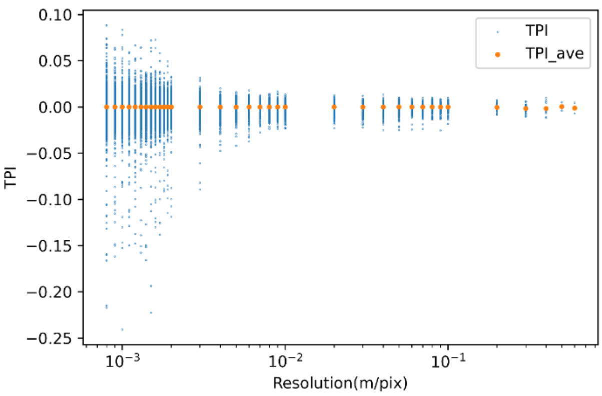


**Figure 14**: - Change of TPI values at different resolutions at Unosaki Coast

*Relationship between HSV color space and ruggedness.* Figure 15 shows the relationship between $G_{TRI}$ and H, S, V at Nogita Coast and Unosaki Coast. The coefficient of determination for V at Unosaki Coast is the highest. The coefficient of determination for V at Nogita Coast is also high. On the other hand, the coefficient of determination for S was very low.

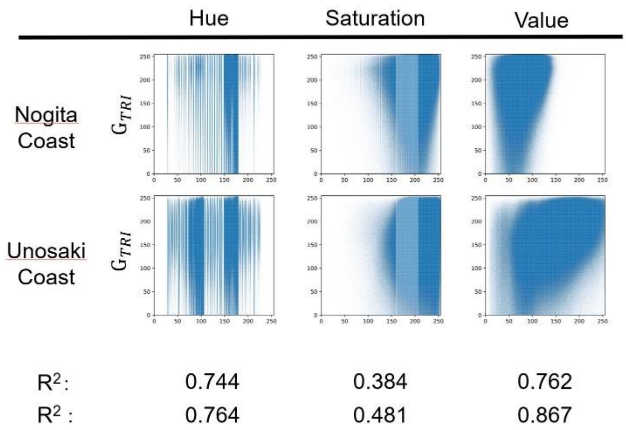


**Figure 15**: - The relationship between $G_{TRI}$ and H, S, V

*Quantifying $G_{TRI}$ by machine learning model.* Figure 16 shows $G_{TRI}$ image quantified by machine learning model and $G_{TRI}$ image calculated based on DEM. At points where the $G_{TRI}$ is large, the roughness is small. On the other hand, at points where the $G_{TRI}$ is small, the roughness is large. Comparing the two images, the locations of the large cracks and roughness are consistent. However, there were differences in the values of $G_{TRI}$.

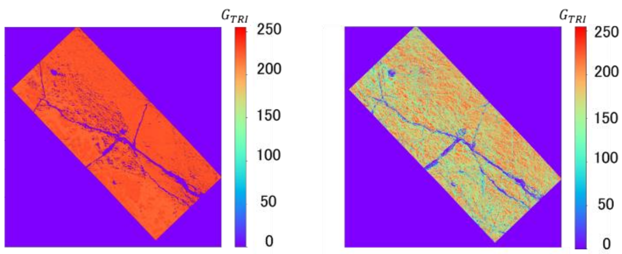


**Figure 16**: - $G_{TRI}$ quantified by machine learning model (left) and $G_{TRI}$ calculated based on DEM (right)

## Discussion

*Change in values of respective ruggedness index with different spatial resolution of DEM.* As the resolution is lowered, the image is smoothed from small ruggedness, so that eventually all the ruggedness is no longer recognizable and the image is considered to be flat. If it were flat, the TRI values would be close to zero, so we would expect the graph to produce a curve that approaches zero as the resolution decreases. However, the maximum value of TRI drops once and then rises within the range of studied spatial resolutions, indicating that The average values of TRI always rise as the resolution becomes coarser. This result is also consistent with our results of Roughness. Because TRI and Roughness use the values of surrounding pixels of given pixel, it is suggested that both TRI and Roughness have increased in both maximum and average values due to the effect of the slope. TPI is zero for the slope, and it is not suitable as an index of ruggedness. Comparing TRI and Roughness, TRI takes higher values in the high-resolution portion. This means that the ruggedness can be checked in more detail. For the above reasons, the most effective index of ruggedness is the TRI.

*Relationship between HSV color space and ruggedness.* The highest coefficient of determination for both the Nogita Coast and Unosaki Coast was for V. In the cracked areas of the outcrop, V is expected to take lower values because of the lack of sunlight, and furthermore, $G_{TRI}$ is expected to take a lower value because of the large unevenness. Therefore, there is a positive correlation between V and $G_{TRI}$. The graphs of H and S show a bias in the values taken by H and S. This may reflect the color of the rock and other factors. This could possibly reflect the color of the rock and other factors. Further study is needed.

*Quantifying $G_{TRI}$ by machine learning model.* Our model could successfully infer the locations of large cracks and large ruggedness, although the numerical agreement was low. The quantified image shows that the flat areas were predicted to be less uneven than they actually are. It is possible that this machine learning model judged the Unosaki Coast to have little ruggedness because they used data from the Nogita Coast, which has a very high degree of ruggedness, as their teacher data. In addition, small ruggedness could not be confirmed in the images quantified by machine learning. This may be due to the fact that our machine learning model was performed using only data from two locations with completely different colors and degrees of ruggedness in this study. We believe that accuracy will be improved if more types of teacher data are used and if teacher data similar to the region to be predicted exist. In this study, MLP was used as the model for machine learning, but it is possible that simply changing to another model could increase accuracy, and improvements to the machine learning model should be considered.

## CONCULUSIONS

In this study, we compared three indexes, TRI, Roughness, and TPI, as quantitative evaluation methods for the surface ruggedness and small-spatial scale roughness of the rock at outcrops by using the data acquired from the two geologically different sites in Japan. TRI and Roughness were found to be suitable as evaluation methods for outcrop surface ruggedness, while TPI was found to be effective in evaluating slope changes, but not in evaluating ruggedness. In terms of changes in spatial resolution, both TRI and Roughness were found to be affected by slope changes. TRI can estimate the surface ruggedness of the rock at outcrops in more detail. We also revealed the relationship between HSV color space and the surface ruggedness of the rock at the outcrop. The correlation between V and $G_{TRI}$ was confirmed, and the use of H revealed the possibility of unique values for different types of rocks and minerals. In addition, a machine learning model was constructed using HSV color space as the explanatory variable and $G_{TRI}$ values as the objective function. Our model could successfully infer $G_{TRI}$ from HSV color space was able to make quantifying. Although improving the accuracy of our model is necessary, our study suggests that we can estimate the small-spatial scale unevenness from 2D images.

## ACKNOWLEDGEMENT

The computation was partly performed on the ITO supercomputer system at the Research Institute for Information Technology of Kyushu University. This work was supported by the Education and Research Program for Mathematical and Data Science from Kyushu University. T.N. acknowledges the financial support from Fukada Field Survey Grants of Fukada Geological Institute.

## REFERENCES

Bemis, S. P., Micklethwaite, S., Turner, D., James, M. R., Akciz, S., T. Thiele, S., & Bangash, H. A. (2014). Ground-based and UAV-Based photogrammetry: A multi-scale, high-resolution mapping tool for structural geology and paleoseismology. *Journal of Structural Geology*, *69*(PA), 163–178. https://doi.org/10.1016/j.jsg.2014.10.007

Blistan, P., Kovanič, Ľ., Zelizňaková, V., & Palková, J. (2016). Using UAV photogrammetry to document rock outcrops. *Acta Montanistica Slovaca*, *21*(2), 154–161.

Buckley, S. J., Ringdal, K., Naumann, N., Dolva, B., Kurz, T. H., Howell, J. A., & Dewez, T. J. B. (2019). LIME: Software for 3-D visualization, interpretation, and communication of virtual geoscience models. *Geosphere*, *15*(1), 222–235. https://doi.org/10.1130/GES02002.1

Google. (2022). *Google Earth*. https://earth.google.com/web/

Koterazawa, R. (1987). Recent Development in Fractography. *Tetsu-to-Hagane*, *73*(1), 19–25. https://doi.org/10.2355/tetsutohagane1955.73.1_19

Li, T., Zhang, B., Xiao, W., Cheng, X., Li, Z., & Zhao, J. (2020). UAV-Based photogrammetry and LiDAR for the characterization of ice morphology evolution. *IEEE Journal of Selected Topics in Applied Earth Observations and Remote Sensing*, *13*, 4188–4199. https://doi.org/10.1109/JSTARS.2020.3010069

Lynch, S. P., & Moutsos, S. (2006). A brief history of fractography. *Journal of Failure Analysis and Prevention*, *6*(6), 54–69. https://doi.org/10.1361/154770206X156231

Nagaya, Y., & Kiku, M. (2020). STUDY ON OPTIMUM CONDITIONS FOR IMPROVING THE MODELING OF STRUCTURES IN UAV-SfM/MVS SURVEY. *Journal of Japan Society of Civil Engineers, Ser. F3 (Civil Engineering Informatics)*, *76*(1), 32–41. https://doi.org/10.2208/jscejcei.76.1_32

Nemoto, T., Raghavan, V., Masumoto, S., & Shiono, K. (2002). Development of SISGeM - An Online System for 3D Geologic Modeling -. *Proceedings of the Open Source GIS - GRASS Users Conference 2002, September*, 11–13.

Riley, S. J., DeGloria, S. D., & Elliot, R. (1999). Terrain_Ruggedness_Index.pdf. In *Intermountain Journal of Science* (Vol. 5, pp. 23–27).

Sato, K., Madokoro, H., Nagayoshi, T., Chiyonobu, S., Martizzi, P., Nix, S., Woo, H., Saito, T. K., & Sato, K. (2021). Semantic Segmentation of Outcrop Images using Deep Learning Networks Toward Realization of Carbon Capture and Storage. *2021 The 21st International Conference on Control, Automation and Systems (ICCAS 2021)*, 11p.

Sato, T., Yamasaki, M., & Chiyonobu, S. (2009). Geology of Akita Prefecture, Japan. *Daichi*, *50*, 70–83.

Totake, Y. (2019). Technologies of digital outcrop model and its application in the petroleum industry. *Journal of the Japanese Association for Petroleum Technology*, *84*(2), 150–159.

Yamada, Y., Masui, R., & Tsuji, T. (2013). Characteristics of a tsunamigenic megasplay fault in the Nankai Trough. *Geophysical Research Letters*, *40*(17), 4594–4598. https://doi.org/10.1002/grl.50888

## ABOUT THE AUTHORS

### Takumu Nakamura

Takumu Nakamura is currently a Master's student at Cooperative Program for Resources Engineering of Kyushu University, Japan. He obtained a Bachelor of Engineering from Department of Earth Resources, Marine and Civil Engineering, School of Engineering, Kyushu University, Japan in March 2022. His research interests include remote sensing, machine learning and VR technologies.

### Arata Kioka

Arata Kioka is currently an Assistant Professor at Department of Earth Resources Engineering, Kyushu University, Japan. Arata earned a Sc.D. degree from Department of Earth and Planetary Sciences, The University of Tokyo, Japan, in 2016. Before joining Kyushu University, he did postdoctoral research at Department of Geocryology of Lomonosov Moscow State University, Russian Federation, Atmosphere and Ocean Research Institute of The University of Tokyo, Japan in 2016, and Institut für Geologie, Fakultät für Geo- und Atmosphärenwissenschaften, Leopold-Franzens Universität Innsbruck, Austria in 2016–2019.

**Yasuhiro Yamada**

Yasuhiro Yamada is a Professor at Department of Earth Resources Engineering, Kyushu University, Japan and a Visiting Professor at Department of Earth Sciences, Royal Holloway University of London, UK, where he obtained a PhD. Before joining Kyushu University in 2021, he worked for the Oil and Gas industry, then was a faculty at Dept of Earth Resources Engineering, Kyoto University, Japan, and a Principal Scientist at JAMSTEC. His research interests include all kinds of subsurface exploration, especially, drilling informatics and its contributions to energy transition.